Overview of the Volume

B.R. Dennis · A.G. Emslie · H.S. Hudson

Abstract In this introductory chapter, we provide a brief summary of the successes and remaining challenges in understanding the solar flare phenomenon and its attendant implications for particle acceleration mechanisms in astrophysical plasmas. We also provide a brief overview of the contents of the other chapters in this volume, with particular reference to the well-observed flare of 2002 July 23.

1 Historical Perspective

This volume of *Space Science Reviews* contains a comprehensive review of our current understanding of the high energy aspects of solar flares. It is written with the same philosophy as the book on solar flares (Sturrock 1980b) that grew out of the *Skylab* workshops. The nine chapters are intended to display the accumulated wisdom of the many scientists who have attended the eleven *RHESSI* (*Reuven Ramaty High Energy Solar Spectroscopic Imager*) science workshops to date. *RHESSI* is a NASA Small Explorer satellite launched in February 2002. The intent was to cover the relevant published literature into 2010, and this succeeded as illustrated in Fig. 1. Results are summarized from hard X-ray and γ-ray observations in Solar Cycle 23 and the complementary observations at other wavelengths that have provided information on the same flares and the often-associated coronal mass ejections (CMEs). We

B.R. Dennis (✉)
Code 671, NASA Goddard Space Flight Center, Greenbelt, MD 20771, USA
e-mail: brian.r.dennis@nasa.gov

A.G. Emslie
Western Kentucky University, Bowling Green, KY 42101, USA
e-mail: emslieg@wku.edu

H.S. Hudson
Space Sciences Laboratory, UC Berkeley, Berkeley, CA 94720, USA
e-mail: hhudson@ssl.berkeley.edu
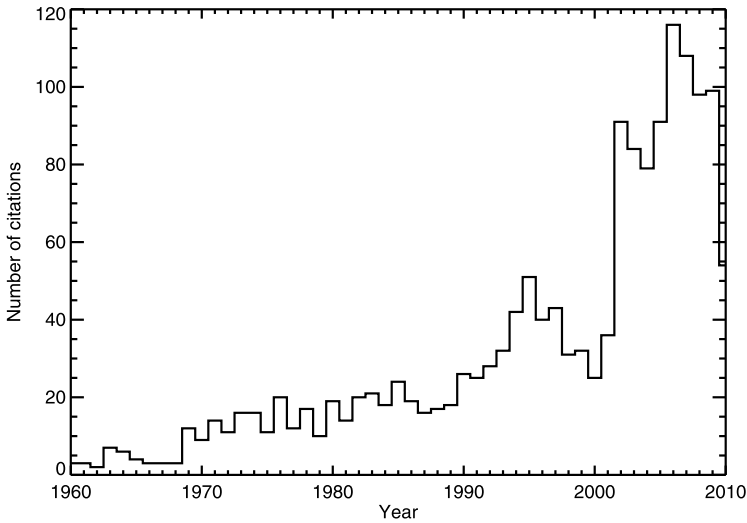
Fig. 1 The distribution by year of the 1,619 (non-unique) citations in Chaps. 1–8 back to 1960; the 20 citations prior to that included papers by Alfvén, Carrington, and Giovanelli among other pioneers. The peak in 2002 coincides with the publication of the initial *RHESSI* results and the peak at around 1995 may be attributable to *Yohkoh* results

anticipate that this volume will be a comprehensive reference of our current state of knowledge and relevant published literature up to the onset of renewed solar activity in Solar Cycle 24.

Although great progress has been made in understanding the solar flare phenomenon since the *Skylab* report, the basic concepts were nevertheless well established at that time from the extensive ground-based observations and early space missions. As summarized by Sturrock (1980a), the basic picture of a flare involved the sudden explosive release of the "free" magnetic energy of a current-carrying magnetic field in the corona. During the flare, the energy would be released by altering (or even destroying) the currents to convert the field to a lower-energy (or even current-free) form. Various energy release mechanisms were considered, including magnetic reconnection, but then, as now, it was recognized that the plasma processes are very complicated and no definitive conclusions could be made on which specific processes were involved.

The acceleration of particles was considered as posing a primary requirement for any flare model. It was recognized though that there was a serious electron "number problem," in that the number of electrons required to explain the measured hard X-ray fluxes was a substantial fraction of the electron content of the corresponding coronal region before the flare. Also, the total power in the 10–100 keV electrons (some 2×10^{29} erg s^{-1} in SOL1972-08-04T06:25 or SOL1972-08-04T06:25)[1] and the total energy contained in these electrons assuming thick-target interactions was known to be an unexpectedly large fraction of the total flare energy (Ramaty et al. 1980). Indeed, Lin and Hudson (1976) had shown that the $\sim$10 to 100 keV electrons "constitute the bulk of the flare energy," perhaps as high as 10 to 50%. This issue remains one of the key problems in understanding the mechanism of

---

[1]In this volume we identify individual flares using the IAU naming convention; see Solar Physics **263**(1) (2010); doi:10.1007/s11207-010-9553-0.

energy release in solar flares as described in Chaps. (3, 7, and 8) of this volume (Holman et al. 2011; Kontar et al. 2011; Zharkova et al. 2011).

The thermal or nonthermal origin of the hard X-ray emission was an ongoing debate in the *Skylab* workshops (Sturrock 1980b). This debate is still not fully resolved (White et al. 2011) but strong support for the nonthermal electron-beam model came with the hard X-ray imaging of the *Solar Maximum Mission (SMM)*, *Hinotori*, and *Yohkoh* satellites. The Hard X-ray Telescope (HXT) on *Yohkoh* produced images of a great many flares (Sato et al. 1999), with the advantage of simultaneous microwave observations (e.g., Bastian et al. 1998; Hannah et al. 2011). The X-ray images revealed the prevalence of double footpoint sources and the near-simultaneity of their light curves to within a second (Sakao et al. 1996). The stronger X-ray source and the weaker radio source both tend to be located in the weaker magnetic field region, consistent with an electron beam model where magnetic mirroring is significant (e.g., Bastian et al. 1998).

The acceleration of ions was also recognized from the γ-ray observations on *OSO-3* (Chupp et al. 1973) and *HEAO-1* (Hudson et al. 1980) but their numbers and energy content were not well understood. It required observations made with the Gamma Ray Spectrometer (Forrest et al. 1980) on *SMM* in the 1980s to reveal that the ions could be accelerated nearly simultaneously with the electrons (Forrest and Chupp 1983) and that the total energy in ions above 1 MeV/nucleon could be comparable to, or even exceed, the total energy in electrons above 20 keV (Ramaty et al. 1995). Similar to electrons (Holman et al. 2011), the total energy content in ions depends to a significant extent on an accurate determination of the low-energy end of the accelerated spectrum, and considerable progress has been made on this front (Vilmer et al. 2011).

The biggest discrepancy between our current understanding of the flare phenomenon and the *Skylab* ideas is in the relationship between flares and coronal mass ejections (CMEs). In the *Skylab* era, CMEs were referred to as coronal transients, and it could still be questioned if they were "incidental to flares or whether they reveal something fundamental about the energy release process" (Rust et al. 1980). It was not until the "solar flare myth" was described by Gosling (1993) that many realized that the CMEs are the major cause of solar effects at the Earth, not the flares as such. This was controversial (Hudson et al. 1995), and with modern data we now understand that flares and energetic CMEs are, in fact, intimately related and may have comparable energy content (Emslie et al. 2004a, 2005) in major events. It is now clear that the largest and fastest CMEs, which have the greatest effect on space weather and pose the greatest danger to satellites, are mostly (possibly always) associated with large flares of comparable total energy. Indeed, the origins and energy sources of flares and CMEs are so intimately entwined that it is impossible to explain one without understanding the other. Thus, if we are to understand these phenomena and develop predictive capabilities, it is imperative that we consider them as interrelated phenomena.

2 Review of Flare Models

It was established very early on in flare studies that the source of the energy released in a flare is in current-carrying (i.e., "non-potential") magnetic fields. Not only are flares invariably connected with magnetism in the photosphere, but an examination of the various candidate sources of energy reveals magnetic energy to be the only plausible contender (Tandberg-Hanssen and Emslie 1988). Release of the energy stored in the twisted magnetic field configuration can proceed through a process termed *magnetic reconnection*, in which the connectivity of the magnetic field redefines itself. However, it is far less clear—and this

is what to a large extent drives flare research—how the energy can be built up *without* reconnection dissipating it immediately, and what "trigger" initiates the flare process. The energy can build up for many hours, or even days, without significant dissipation of the energy prior to the flare onset.

Sturrock (1980a) provided a concise, yet thorough, review of the various reconnection scenarios that existed through the end of the 1970s. In fairness, it must be conceded that most of these scenarios are still valid, although many have fallen out of favor. Perhaps the most significant "casualty" is the model of Gold and Hoyle (1960), which invoked the self-attraction of magnetic loops carrying parallel, or near-parallel, currents, leading to an energy release at their mutual interface. While this laboratory analogy is rather appealing, it unfortunately fails to recognize that it is not currents that attract *per se*, but rather one current interacts with the magnetic field produced by the other. Thus, in the global force-free field appropriate to the low-β solar corona, the current density $\mathbf{J}$ is always nearly parallel to the local magnetic field $\mathbf{B}$, and no $\mathbf{J} \times \mathbf{B}$ force exists. Independent magnetic flux loops therefore have no particular attraction to (or repulsion from) each other, and some external influence (such as a photospheric velocity field; e.g. Heyvaerts et al. 1977) must be postulated in order to drive them together.

Basic Sweet-Parker reconnection (e.g., Sweet 1969), has also fallen out of favor because it is perceived to develop too slowly. In its place Petschek reconnection, which is both much faster and is characterized by energy release at reconnection-driven shocks (Petschek 1964) rather than at the point of reconnection, has appeared in many descriptions. The standard "CSHKP" (Carmichael 1964; Sturrock 1966; Hirayama 1974; Kopp and Pneuman 1976) model, suggested by the growth of soft X-ray "loop prominence systems" accompanying the increasing separation of Hα "ribbons," invokes a reconnection site near the apex of the loop system. This injects energy (e.g., as flows) into the underlying loops. Although this model does not naturally account for the impulsive phase of a flare, nor the particle acceleration, a great deal of effort has been expended in quantitative modeling of such structures (density of loop-top source, standing shocks in loop legs, etc.). Aspects of these problems are discussed in Zharkova et al. (2011).

The planning of the *RHESSI* workshop series addressed the need to consider the physics of magnetic reconnection, and the concomitant acceleration of electrons and ions, *in the context of the observations*. For example, it was recognized early on that "test-particle" approaches to particle acceleration, in which the electric and magnetic fields are *prescribed* and constant in time, do not adequately take into account the fact that the mass, momentum, energy, and electrical current carried by the large number of accelerated particles necessary to account for flare observations must have a major feedback on both the electrodynamic and magnetohydrodynamic environments of the acceleration region. A major emphasis of the theory team (Zharkova et al. 2011) at the *RHESSI* workshops was the development of acceleration models that explicitly take these nonlinear aspects of the process into account.

3 Challenges for Simple Acceleration Models

The impulsive phase of a solar flare is characterized, in part, by the emission of a copious flux of hard X-rays (photon energy $\varepsilon \gtrsim 10$ keV). It is generally accepted that these hard X-rays are produced by collisional bremsstrahlung (free-free emission) when accelerated electrons encounter ambient protons and heavier ions in the solar atmosphere, although other emission mechanisms have also been considered (Kontar et al. 2011). The amount of electron energy required to produce these hard X-rays depends on the model used to characterize the interaction of the accelerated electrons with the target. A lower limit is given by a

collisional thick-target interpretation (e.g., Brown 1971), in which all of the electron energy is absorbed in the target only through Coulomb collisions with ambient particles (primarily electrons). In this interpretation, the ratio of electron power to emitted hard X-ray power is of order 10^5 (see (4.4) below), and this gives an order-of-magnitude estimate for the rate of electron acceleration in the flare (Holman et al. 2011). For a large (e.g., *GOES* X-class) flare, the required rate of acceleration of electrons above 20 keV can exceed 10^{37} s^{-1}, a large number with interesting consequences (e.g., Miller et al. 1997), as we now discuss.

First, the number of electrons $\mathcal{N}$ confined in the coronal portion of a flare loop is simply the number density n (cm^{-3}) multiplied by the volume V (cm^3). Inserting typical values $n \approx 10^{11}$ and $V \approx 10^{27}$ gives $\mathcal{N} \approx 10^{38}$, so that the acceleration process would deplete the store of available electrons in 10 s or so, significantly less than the observed duration of the flare. This simple calculation therefore rules out models in which all the electrons to be accelerated are stored in a coronal volume prior to the onset of the flare. If the acceleration site is indeed in the corona, this requires instead that the electrons "recycle" multiple times or that fresh electrons enter from the chromosphere. Given that electrons in the solar atmosphere have gyroradii of order a centimeter and so are strongly tied to the guiding magnetic field lines, this presents formidable difficulties for current closure of the accelerated electron streams. Although solutions to this problem have been offered (Emslie and Hénoux 1995), they require the synergistic interaction of a large number ($\sim 10^{10}$ or so) of separate acceleration regions, and the origin (not to mention stability) of such a system has yet to be adequately explored.

Second, the accelerated electrons carry with them an associated *electrical current* of some 10^{18} A (3×10^{27} statamps). In steady-state, such a current, if assumed to propagate unidirectionally in a flux tube of radius 10^9 cm, gives rise, via Ampère's Law, to a magnetic field $B \approx 2 \times 10^8$ Gauss. Not only is such a high magnetic field completely untenable on observational grounds, the associated energy density $B^2/8\pi \approx 10^{15}$ erg cm^{-3}, for a total energy content $\int (B^2/8\pi)\, dV$ of some 10^{42} ergs, some ten orders of magnitude larger than the energy content in the electron beam that ostensibly produces the field, even for a 1000-second beam.

Third, a current of this magnitude cannot appear instantaneously. The self-inductance $\mathcal{L}$ of a structure scales with ℓ, the characteristic dimension. For a solar flare loop of typical dimensions, we find $\mathcal{L} \approx 10$ H. Hence, to initiate a current $I \approx 10^{18}$ A in a time $\tau \approx 10$ s requires a voltage $V \approx \mathcal{L}I/\tau \approx 10^{18}$ V, which is *fourteen* orders of magnitude higher than the typical energy of the accelerated electrons.

Such considerations have led various authors (e.g., Knight and Sturrock 1977; Emslie 1980; Brown and Bingham 1984; Spicer and Sudan 1984; Larosa and Emslie 1989; van den Oord 1990; Zharkova et al. 1995) to consider models in which cospatial return currents locally neutralize the beam current. However, such models can only produce beam-current neutralization in the *propagation* region, and considerable analysis has been performed on the details of the beam/return current interaction in this propagation region (van Oss and van den Oord 1995). In the acceleration region itself, return-current electrons would have to flow in a direction counter to the applied electromotive force and so cannot neutralize the unacceptably large currents therein. Although significant progress on this issue has been made recently (Zharkova et al. 2011), a satisfactory resolution of this issue has yet to be offered. A self-consistent electrodynamic theory would require a description of current closure in the acceleration region as well as in the beam itself. This difficulty has led various authors to reject acceleration models featuring large-scale electric fields in favor either of acceleration by very large electric fields in localized current sheets, or via acceleration in (stochastic) MHD or plasma waves.

The problems imposed by the return current become more severe as the beam becomes more intense. It has become increasingly clear directly from *RHESSI* imaging (e.g., Dennis and Pernak 2009) that the hypothetical electron beam would occupy only a small area. Closely related emissions such as UV and white light are often unresolved at even higher resolution and suggest areas substantially smaller than 10^{16} cm^2 (Fletcher et al. 2011). Accordingly, alternatives that replace electron-beam energy transport with Poynting fluxes have been proposed (Emslie and Sturrock 1982; Haerendel 2006; Fletcher and Hudson 2008; Haerendel 2009).

4 Importance of Hard X-Rays and γ-Rays as Diagnostics of Accelerated Particles

It is important to emphasize that the energy released as hard X-rays and γ-rays is—in and of itself—a negligible component of that released in the flare. The importance of this radiation lies not in its energy content *per se*, but rather in the energy in accelerated particles required to produce this diagnostic radiation (Holman et al. 2011; Vilmer et al. 2011).

The process of hard X-ray emission is very inefficient. In order to produce a photon by bremsstrahlung, an electron must suffer a near-direct collision on an ambient ion. Most electrons instead lose their energy in a large number of small-angle scatterings off ambient electrons, and do not contribute to the bremsstrahlung yield. We may compare the energy emitted through bremsstrahlung to that suffered in Coulomb collisions by comparing the cross-sections for the two processes. The nonrelativistic differential cross-section (cm^2 per unit photon energy) for free-free emission of a photon of energy ε by an electron of energy E may be, to order-of-magnitude, approximated by the Kramers form

$$\sigma(\varepsilon, E) \approx \alpha \frac{r_o^2 mc^2}{\varepsilon E}, \tag{4.1}$$

where $\alpha \approx 1/137$ is the fine structure constant, $mc^2 = 511$ keV is the electron rest mass, and r_0 is the classical radius of the electron. From this it follows that the cross-section (cm^2 keV) for energy loss through bremsstrahlung by an electron of energy E is

$$\sigma_E^B = \int_0^E \varepsilon \sigma(\varepsilon, E) \, dE \approx \alpha r_o^2 mc^2. \tag{4.2}$$

By contrast, the cross-section for Coulomb energy loss (cm^2 keV) by an electron of energy E is (Brown 1972; Emslie 1978)

$$\sigma_E^C(\varepsilon, E) = \frac{2\pi e^4 \Lambda}{E} \approx \Lambda \frac{r_o^2 (mc^2)^2}{E}, \tag{4.3}$$

where Λ is the Coulomb logarithm, ε is the electron charge, and we have used $r_o = e^2/mc^2$. Taking the ratio

$$\eta = \frac{\sigma_E^B}{\sigma_E^C} \approx \frac{\alpha}{\Lambda} \frac{E}{mc^2} \approx 4 \times 10^{-4} \frac{E}{mc^2} \tag{4.4}$$

gives the energetic efficiency of the bremsstrahlung process relative to Coulomb collisions. For $E \approx 20$ keV, $\eta \approx 1.5 \times 10^{-5}$, i.e., for each erg of bremsstrahlung, $\gtrsim 10^5$ ergs of energy in electrons are required.

Gamma-rays in solar flares (Vilmer et al. 2011) are produced principally by the interaction of accelerated protons and heavier ions with nuclei in the ambient atmosphere, although electron-ion bremsstrahlung from accelerated electrons can also contribute. Unlike hard X-ray emission, not all γ-ray emission is prompt—in particular, the capture of neutrons onto ambient protons to create the 2.223 MeV deuterium-formation line can take several minutes because of the need to reduce the momentum of the neutrons to a value where the cross-section for recombination is sufficiently high. The low speed of the captured neutrons also leads to the extremely small spectral width of the 2.223 MeV line; by contrast, most γ-ray lines (e.g., the prompt nuclear de-excitation lines of ^{12}C at 4.4 MeV and ^{16}O at 6.1 MeV) have both narrow and broad spectral profiles depending on whether the heavy ions are the target or the projectile in interactions with accelerated or ambient protons, respectively.

RHESSI not only provides γ-ray spectra with unprecedented spectral resolution (Smith et al. 2003) but also, on a few occasions, *images* of the γ-ray line emission—in particular in the 2.223 MeV line. Interestingly, the locations of the hard X-ray and γ-ray sources are *not* coincident (Hurford et al. 2003, 2006), indicating a preferential acceleration of electrons vs. protons in different substructures within the flare volume (cf. Emslie et al. 2004b).

Some time after the publication of the *Skylab* volume, studies of observations from the *SMM* Gamma-Ray Spectrometer (GRS) (Share and Murphy 1995) led Ramaty et al. (1995) to realize that the spectra of the accelerated ions could remain steep down to energies as low as 1 MeV, and hence that the *energy content* of accelerated ions in solar flares, as revealed by their γ-ray emission, could rival that of the accelerated electrons, hitherto thought to dominate the energy budget of accelerated particles. Further study of the relative partitioning of energy between accelerated electrons and ions was carried out by Emslie et al. (2004a, 2005), who reached a similar conclusion. Further discussion of the partitioning of flare energy amongst its constituent parts can be found in Fletcher et al. (2011), Holman et al. (2011), and Vilmer et al. (2011).

5 *RHESSI* Design and Capabilities

5.1 Operations

RHESSI (Lin et al. 2002) uses nine cooled and segmented germanium detectors to achieve high-resolution X-ray and γ-ray spectroscopy across the full energy range from 3 keV to 17 MeV (Smith et al. 2002). The FWHM energy resolution increases from ~1 keV at the lowest energies to ~10 keV at the highest. This has proved adequate to detect the iron-line complex at ~6.7 keV, measure the steep hard X-ray continuum spectra with relative flux accuracies as fine as 1%, measure the width of the positron-annihilation line at 511 keV as it varies with time during a flare, and resolve all of the narrow nuclear γ-ray lines except for the intrinsically narrow neutron-capture line at 2.223 MeV. A bi-grid tungsten collimator over each detector modulates the incident photon flux as the spacecraft rotates at ~15 rpm to provide the temporal information needed for the Fourier-transform technique that is used to reconstruct the X-ray and γ-ray images (Hurford et al. 2002). Imaging is possible at all energies up to about 1 MeV, with an angular resolution of ~2″ (FWHM) up to ~100 keV increasing to ~20″ at 1 MeV. When the count rates are sufficiently high, images can be made with a cadence as short as 4 s. In addition, images can also be made in the neutron-capture γ-ray line at 2.223 MeV in the relatively few flares when the total number of photons detected in this line is sufficiently high (several thousand; Hurford et al. 2006). The field of view is ~1°, and so a flare can be imaged no matter where on the visible disk it occurs. *RHESSI*

has an effective sensitive area that reaches ∼60 cm^2 at 100 keV. Two thin aluminum disks can be automatically moved above each detector to attenuate intense soft X-ray fluxes so that *RHESSI* can operate with minimal detector saturation and pulse pile-up over a wide dynamic range in flux level. This allows coverage of both faint microflares (with the attenuators removed) and the most powerful flares (with both attenuators in place over each detector).

   RHESSI was launched on 2002 February 5 and has been in operation almost continuously since 2002 February 11, with brief intervals of pointing away from the Sun for observations of the Crab Nebula and solar global emission (the quiet Sun as a star). The *GOES* class X4.8 flare SOL2002-07-23T00:35 yielded the first γ-ray emission lines detected by *RHESSI* (see Shih et al. 2009 for a summary of all γ-ray events seen with *RHESSI* as of the Cycle 23/Cycle 24 solar minimum). By the time of writing, there have been two successful *anneals* of the germanium detectors, in November 2007 and again in April 2010. These are month-long procedures needed to restore sensitive volume and energy resolution that become degraded by the accumulation of radiation damage.

5.2 Collaborations

Because solar flares and other forms of activity are defined by particle acceleration and extreme heating, *RHESSI* observations are at the heart of many broader studies. Instruments on other spacecraft and at ground-based observatories around the world have been active participants in providing the magnetic, thermal, and dynamic context in which the X-ray and γ-ray sources are produced. In addition, microwave observations of the gyrosynchrotron emission provide additional information on the accelerated electrons themselves. Coronagraph observations of CMEs, and *in situ* particle-and-field measurements in the near-Earth environment, also provide information that can be used to establish the links between these related phenomena and any associated flares. A partial list of all collaborating space-based observatories with further information can be found on the Max Millennium Web site at http://solar.physics.montana.edu/max_millennium/obs/SBO.html. They include the *ACE, Cluster, CORONAS, GOES, INTEGRAL, SOHO, TRACE*, and *WIND* spacecraft. More recently, complementary observations have been made with the newer solar missions including *Hinode*, *STEREO*, *SDO*, and *Fermi*. They have provided X-ray, EUV, UV, optical, and *in situ* particle-and-field measurements relevant to the many events recorded by *RHESSI*. Thanks to the daily email messages and the coordinating efforts of the Max Millennium program, many collaborative observing campaigns have been conducted to maximize the overlap of the various observatory programs.

6 Outline of This Volume

The contents of this volume center on *RHESSI* capabilities and research flowing from the *RHESSI* data, but this embraces most of flare physics because of the dominating importance of the high-energy processes. The current volume consists of a series of articles, each representing the work of multiple authors. The purpose of each article is to present a review of the pertinent subject matter, linking the results of a variety of published works into a coherent whole, which we hope is useful both for the reader who wishes an overview of contemporary knowledge in the area, and for the experienced researcher to view results in context. Each article presents mid-length reviews of the literature, and provides a comprehensive reference list for the reader who seeks more detailed developments or information.

Taken as a whole, the Editors hope that this volume will be a useful successor for the *Skylab* workshop volume (Sturrock 1980b), and we hope that Zharkova et al. (2011) in particular will play the same role for solar-flare particle acceleration as reviewed earlier by Miller et al. (1997).

Although each of the articles presents a somewhat different aspect of solar flare research, they are all inter-related and should be read in this context. To illustrate the inter-relationship of these articles, we note that much attention has been paid to the characteristics of the first γ-ray line flare detected with *RHESSI* mentioned above (SOL2002-07-23T00:35) This event forms the basis for much of the discussion in each article, namely:

- The temporal, spatial and spectral properties of the intense hard X-ray radiation from this flare are discussed in Kontar et al. (2011); this includes a discussion of the temporal evolution of the hard X-ray spectrum, both for the flare as a whole and for subregions (e.g., coronal sources, chromospheric footpoints) observed within the active region. Using an appropriate cross-section for hard X-ray production, regularized spectral inversion of the observed hard X-ray spectrum then yields the volume-averaged mean source electron spectrum for the event.
- A useful check on the electron spectrum comes from observations of deka-GHz radio emission (White et al. 2011); this radio emission is believed to be produced by the high-energy tail of the same ensemble of electrons that produces the deka-keV hard X-ray emission, but the inferred electron spectra are intriguingly different.
- As discussed in Holman et al. (2011), combining the mean source electron spectrum with an appropriate electron transport model then leads to the *accelerated* electron spectrum. Analysis of this accelerated spectrum (with particular attention to the low-energy end where, due to the typically steep spectra involved, most of the particle energy resides) then yields information on the total energy in the accelerated electrons.
- Vilmer et al. (2011) discuss various aspects of the γ-ray emission from this event. It includes a comparison of the time profiles and spatial locations of hard X-ray and γ-ray sources. The intensity and Doppler shifts of the γ-ray lines are also presented along with the information that these measurements provide on the number and angular distribution of accelerated ions, and even on the magnetic field geometry in the active region.
- Results from all photon energy ranges (hard X-ray, soft X-ray, γ-ray, optical and EUV) are synthesized into a global picture of the energetics of this flare in Fletcher et al. (2011).
- The position of this flare within the statistical ensemble of all flare events detected with *RHESSI*, extending from B-class microflares to large X-class events, is provided in Hannah et al. (2011).
- Zharkova et al. (2011) review the implications of these observational results for theoretical models of particle acceleration and transport in flare plasmas, and in the broader field of acceleration in astrophysical sources.
- Lin (2011) summarizes these results and presents prospects for future research directions.

Appendix: Glossary of Acronyms Used in the Monograph

3DP   3-D Particles, onboard *WIND*

AAS   American Astronomical Society
ACE   *Advanced Composition Explorer*

ACRIM	Active Cavity Radiometer Irradiance Monitor, onboard *SMM*
AIA	Atmospheric Imaging Assembly, onboard *SDO*
ARTB	active-region transient brightening
ATST	Advanced Technology Solar Telescope
BATSE	Burst And Transient Source Experiment, onboard *CGRO*
BBSO	Big Bear Solar Observatory
BCS	Bent or Bragg Crystal Spectrometer, onboard *SMM* or *Yohkoh*
CA	cellular automaton
CCD	charge-coupled device
CDF	cumulative distribution function
CDS	Coronal Diagnostic Spectrometer, onboard *SoHO*
CGRO	*Compton Gamma Ray Observatory*
CME	coronal mass ejection
COMPTEL	Imaging Compton Telescope, onboard *CGRO*
CoMP	Coronal Multi-channel Polarimeter
CORONAS	*Complex ORbital ObservatioNs of the Active Sun* satellite series
CoSMO	Coronal Solar Magnetism Observatory
CSHKP	Carmichael, Sturrock, Hirayama, Kopp & Pneuman flare model
DC	direct current
DEM	differential mission measure
DOI	Digital Object Identifier
DR	diffusion region
EDF	empirical distribution function
EIS	EUV Imaging Spectrometer, onboard *Hinode*
EIT	Extreme ultraviolet Imaging Telescope, onboard *SoHO*
EM	emission measure
ENA	energetic neutral atom
EP	erupting prominence
ESA	European Space Agency
EST	European Solar Telescope
EUV	extreme ultraviolet
EVE	EUV Variability Experiment, onboard *SDO*
FAL	Fontenla, Avrett, & Loeser solar atmospheric model
FASR	Frequency Agile Solar Radiotelescope
FIP	first ionization potential
FMSS	fast-mode standing shock
FOXSI	Focusing Optics hard X-ray Spectrometer Imager
FP	footpoint
FWHM	full width at half maximum
GBM	Gamma-ray Burst Monitor, onboard *Fermi*
GeDs	germanium detectors
GEM	Geospace Environment Modeling
GLE	ground-level event

GOES	*Geostationary Operational Environmental Satellite*
GONG	Global Oscillation Network Group
GRANAT	*Gamma Rentgenovskii Astronomicheskii Nauchni ApparaT*
GRB	gamma-ray burst
GRIPS	*Gamma-Ray Imaging Polarimeter for Solar flares*
GRS	Gamma Ray Spectrometer, onboard *SMM*
GSAT-2	Geostationary Satellite launched by the Indian Space Research Organization on May 8, 2003
GSFC	[NASA] Goddard Space Flight Center
HEAO	*High Energy Astrophysical Observatory* satellite series
HMI	Helioseismic and Magnetic Imager, onboard *SDO*
HXIS	Hard X-ray Imaging Spectrometer, onboard *SMM*
HXR	hard X-ray
HXRBS	Hard X-Ray Burst Spectrometer, onboard *SMM*
HXRS	Hard X-ray Spectrometer, onboard *MTI*
HXT	Hard X-ray Telescope, onboard *Yohkoh*
IAU	International Astronomical Union
ICE	*International Cometary Explorer*, a.k.a *ISEE-3*
ICME	interplanetary coronal mass ejection
IDL	Interactive Data Language
IGY	International Geophysical Year
INTEGRAL	*INTErnational Gamma-Ray Astrophysics Laboratory*
IR	infrared
ISEE	*International Sun-Earth Explorer* satellite series
KOSMA	Kölner Observatorium für SubMillimeter Astronomie
KS	Kolmogorov-Smirnov statistic
LASCO	Large Angle and Spectrometric Coronagraph, onboard *SoHO*
LDE	long-decay event
LHDI	lower hybrid drift instability
LOFAR	Low Frequency Array for Radio Astronomy
LOS	line-of-sight
LPF	large proton flare
LTE	local thermal equilibrium
MDI	Michelson Doppler Imager, onboard *SoHO*
MEKAL	Mewe-Kaastra-Liedahl atomic code
MEM	maximum entropy method
MESSENGER	*MErcury Surface, Space ENvironment, GEochemistry, and Ranging* mission
MHD	magnetohydrodynamic(s)
MISS	Multichannel Infrared Solar Spectrograph, at PMO
MSFC	[NASA] Marshall Space Flight Center
MTI	*Multi-Thermal Imager*
NASA	National Aeronautics and Space Administration

NOAA	National Oceanic and Atmospheric Administration
NoRH	Nobeyama Radioheliograph
NoRP	Nobeyama Radio Polarimeters
NRBH	nonrelativistic Bethe-Heitler (bremsstrahlung cross-section)
NRH	Nançay Radioheliograph
OSO	*Orbiting Solar Observatory* satellite series
OSPEX	Object SPectral EXecutive (IDL-based spectral analysis software)
OSSE	Oriented Scintillation Spectrometer Experiment, onboard *CGRO*
OVSA	Owens Valley Solar Array
PA	position angle
PASJ	Publications of the Astronomical Society of Japan
PDF	probability density function
PFL	post-flare loop
PHEBUS	Payload for High Energy BUrst Spectroscopy, onboard *GRANAT*
PIC	particle-in-cell
PIL	polarity inversion line
PMO	Purple Mountain solar Observatory
POLAR	*POLAR* spacecraft, not an acronym
PVO	*Pioneer Venus Orbiter*
QPP	quasi-periodic pulsations
RCS	reconnecting current sheet
RESIK	REntgenovsky Spektrometr s Izognutymi Kristalami, onboard *CORONAS-F*
RHESSI	*Reuven Ramaty High Energy Solar Spectroscopic Imager*
RMC	rotation modulation collimator
SC	(*RHESSI*) subcollimators
SDO	*Solar Dynamics Observatory*
SEE	*Solar Eruptive Events*
SEP	solar energetic particle
SFU	solar flux unit (10^{-22} W m^{-2} Hz^{-1})
SHH	soft-hard-harder (temporal behavior of spectral index)
SHS	soft-hard-soft (temporal behavior of spectral index)
SIGMA	Systéme d'Imagerie Gamma à Masque Aléatoire, instrument onboard *GRANAT*
SMART	Hida Solar Magnetic Activity Research Telescope
SMM	*Solar Maximum Mission*
SMSS	slow-mode standing shock
SOC	self-organized criticality
SOHO or *SoHO*	*Solar and Heliospheric Observatory*
SOLIS	Synoptic Optical Long-term Investigations of the Sun magnetograph
SONG	SOlar Neutrons and Gamma-rays instrument, onboard *CORONAS-F*
SORCE	*Solar Radiation and Climate Experiment*
SOT	Solar Optical Telescope, onboard *Hinode*

SOXS	SOlar X-ray Spectrometer, onboard *GSAT-2*
SPI	SPectrometer on Integral, onboard *INTEGRAL*
SPR-N	Solar Spectropolarimeter, onboard *CORONAS-F*
SSRT	Siberian Solar Radio Telescope
SST	Solar Submillimeter Telescope
ST	Hubble Space Telescope
STEREO	*Solar TErrestrial RElations Observatory*
SUMER	Solar Ultraviolet Measurements of Emitted Radiation instrument, onboard *SoHO*
SXI	Soft X-ray Imager, onboard *GOES*
SXR	soft X-ray
SXT	Soft or Solar X-ray Telescope, onboard *Yohkoh* or *Hinotori*, respectively
THEMIS	*Time History of Events and Macroscale Interactions during Substorms*
TIM	Total Irradiance Monitor, onboard *SORCE*
TOF	time-of-flight
TRACE	*Transition Region and Coronal Dynamics Explorer*
TS	termination shock
TSI	total solar irradiance
UV	ultraviolet
UVCS	Ultraviolet Coronagraph Spectrometer, onboard *SoHO*
VAL	Vernazza, Avrett, & Loeser solar atmospheric model
VLA	Very Large Array
VUV	vacuum ultraviolet
WATCH	Wide Angle Telescope for Cosmic Hard X-rays; onboard *GRANAT*
WAVES	Not an acronym; instrument onboard *WIND*
WBS	Wide Band Spectrometer, onboard *Yohkoh*
WIND	Spacecraft; not an acronym
WL	white light
XBP	X-ray bright point
XRT	X-Ray Telescope, onboard *Hinode*
XUV	X-ray/EUV/UV

References

T.S. Bastian, A.O. Benz, D.E. Gary, Annu. Rev. Astron. Astrophys. **36**, 131 (1998)

J.C. Brown, Sol. Phys. **18**, 489 (1971)

J.C. Brown, Sol. Phys. **26**, 441 (1972)

J.C. Brown, R. Bingham, Astron. Astrophys. **131**, L11 (1984)

H. Carmichael, NASA Spec. Publ. **50**, 451 (1964)

E.L. Chupp, D.J. Forrest, P.R. Higbie, A.N. Suri, C. Tsai, P.P. Dunphy, Nature **241**, 333 (1973)

B.R. Dennis, R.L. Pernak, Astrophys. J. **698**, 2131 (2009)

A.G. Emslie, Astrophys. J. **224**, 241 (1978)

A.G. Emslie, Astrophys. J. **235**, 1055 (1980)

A.G. Emslie, B.R. Dennis, G.D. Holman, H.S. Hudson, J. Geophys. Res. **110**, 11103 (2005)

A.G. Emslie, J.-C. Hénoux, Astrophys. J. **446**, 371 (1995)

A.G. Emslie, H. Kucharek, B.R. Dennis, N. Gopalswamy, G.D. Holman, G.H. Share, A. Vourlidas, T.G. Forbes, P.T. Gallagher, G.M. Mason, T.R. Metcalf, R.A. Mewaldt, R.J. Murphy, R.A. Schwartz, T.H. Zurbuchen, J. Geophys. Res. **109**, 10104 (2004a)
A.G. Emslie, J.A. Miller, J.C. Brown, Astrophys. J. Lett. **602**, L69 (2004b)
A.G. Emslie, P.A. Sturrock, Sol. Phys. **80**, 99 (1982)
L. Fletcher, H.S. Hudson, Astrophys. J. **675**, 1645 (2008)
L. Fletcher et al., Space Sci. Rev. (2011). doi:10.1007/s11214-010-9701-8
D.J. Forrest, E.L. Chupp, Nature **305**, 291 (1983)
D.J. Forrest, E.L. Chupp, J.M. Ryan, M.L. Cherry, I.U. Gleske, C. Reppin, K. Pinkau, E. Rieger, G. Kanbach, R.L. Kinzer, Sol. Phys. **65**, 15 (1980)
T. Gold, F. Hoyle, Mon. Not. R. Astron. Soc. **120**, 89 (1960)
J.T. Gosling, J. Geophys. Res. **98**, 18937 (1993)
G. Haerendel, Space Sci. Rev. **124**, 317 (2006)
G. Haerendel, Astrophys. J. **707**, 903 (2009)
I. Hannah et al., Space Sci. Rev. (2011)
J. Heyvaerts, E.R. Priest, D.M. Rust, Astrophys. J. **216**, 123 (1977)
T. Hirayama, Sol. Phys. **34**, 323 (1974)
G. Holman et al., Space Sci. Rev. (2011). doi:10.1007/s11214-010-9680-9
H. Hudson, B. Haisch, K.T. Strong, J. Geophys. Res. **100**, 3473 (1995)
H.S. Hudson, T. Bai, D.E. Gruber, J.L. Matteson, P.L. Nolan, L.E. Peterson, Astrophys. J. Lett. **236**, L91 (1980)
G.J. Hurford, S. Krucker, R.P. Lin, R.A. Schwartz, G.H. Share, D.M. Smith, Astrophys. J. Lett. **644**, L93 (2006)
G.J. Hurford, E.J. Schmahl, R.A. Schwartz, A.J. Conway, M.J. Aschwanden, A. Csillaghy, B.R. Dennis, C. Johns-Krull, S. Krucker, R.P. Lin, J. McTiernan, T.R. Metcalf, J. Sato, D.M. Smith, Sol. Phys. **210**, 61 (2002)
G.J. Hurford, R.A. Schwartz, S. Krucker, R.P. Lin, D.M. Smith, N. Vilmer, Astrophys. J. Lett. **595**, L77 (2003)
J.W. Knight, P.A. Sturrock, Astrophys. J. **218**, 306 (1977)
E. Kontar et al., Space Sci. Rev. (2011). doi:10.1007/s11214-011-9804-x
R.A. Kopp, G.W. Pneuman, Sol. Phys. **50**, 85 (1976)
T.N. Larosa, A.G. Emslie, Sol. Phys. **120**, 343 (1989)
R. Lin, Space Sci. Rev. (2011). doi:10.1007/s11214-011-9801-0
R.P. Lin, B.R. Dennis, G.J. Hurford, D.M. Smith, A. Zehnder, P.R. Harvey, D.W. Curtis, D. Pankow, P. Turin, M. Bester, A. Csillaghy, M. Lewis, N. Madden, H.F. van Beek, M. Appleby, T. Raudorf, J. McTiernan, R. Ramaty, E. Schmahl, R. Schwartz, S. Krucker, R. Abiad, T. Quinn, P. Berg, M. Hashii, R. Sterling, R. Jackson, R. Pratt, R.D. Campbell, D. Malone, D. Landis, C.P. Barrington-Leigh, S. Slassi-Sennou, C. Cork, D. Clark, D. Amato, L. Orwig, R. Boyle, I.S. Banks, K. Shirey, A.K. Tolbert, D. Zarro, F. Snow, K. Thomsen, R. Henneck, A. Mchedlishvili, P. Ming, M. Fivian, J. Jordan, R. Wanner, J. Crubb, J. Preble, M. Matranga, A. Benz, H. Hudson, R.C. Canfield, G.D. Holman, C. Crannell, T. Kosugi, A.G. Emslie, N. Vilmer, J.C. Brown, C. Johns-Krull, M. Aschwanden, T. Metcalf, A. Conway, Sol. Phys. **210**, 3 (2002)
R.P. Lin, H.S. Hudson, Sol. Phys. **50**, 153 (1976)
J.A. Miller, P.J. Cargill, A.G. Emslie, G.D. Holman, B.R. Dennis, T.N. LaRosa, R.M. Winglee, S.G. Benka, S. Tsuneta, J. Geophys. Res. **102**, 14631 (1997)
H.E. Petschek, NASA Spec. Publ. **50**, 425 (1964)
R. Ramaty, N. Mandzhavidze, B. Kozlovsky, R.J. Murphy, Astrophys. J. Lett. **455**, L193+ (1995)
R. Ramaty, C. Paizis, S.A. Colgate, G.A. Dulk, P. Hoyng, J.W. Knight, R.P. Lin, D.B. Melrose, F. Orrall, P.R. Shapiro, in *Skylab Solar Workshop II*, ed. by P.A. Sturrock (1980), pp. 117–185
D.M. Rust, E. Hildner, R.T. Hansen, M. Dryer, A.N. McClymont, S.M.P. McKenna-Lawlor, D.J. McLean, E.J. Schmahl, R.S. Steinolfson, E. Tandberg-Hanssen, in *Skylab Solar Workshop II*, ed. by P.A. Sturrock (1980), pp. 273–339
T. Sakao, T. Kosugi, S. Masuda, K. Yaji, M. Inda-Koide, K. Makishima, Adv. Space Res. **17**, 67 (1996)
J. Sato, T. Kosugi, K. Makishima, Publ. Astron. Soc. Jpn. **51**, 127 (1999)
G.H. Share, R.J. Murphy, Astrophys. J. **452**, 933 (1995)
A.Y. Shih, R.P. Lin, D.M. Smith, Astrophys. J. Lett. **698**, L152 (2009)
D.M. Smith, R.P. Lin, P. Turin, D.W. Curtis, J.H. Primbsch, R.D. Campbell, R. Abiad, P. Schroeder, C.P. Cork, E.L. Hull, D.A. Landis, N.W. Madden, D. Malone, R.H. Pehl, T. Raudorf, P. Sangsingkeow, R. Boyle, I.S. Banks, K. Shirey, R. Schwartz, Sol. Phys. **210**, 33 (2002)
D.M. Smith, G.H. Share, R.J. Murphy, R.A. Schwartz, A.Y. Shih, R.P. Lin, Astrophys. J. Lett. **595**, L81 (2003)

D.S. Spicer, R.N. Sudan, Astrophys. J. **280**, 448 (1984)

P.A. Sturrock, Nature **211**, 695 (1966)

P.A. Sturrock, in *Skylab Solar Workshop II*, ed. by P.A. Sturrock (1980a), pp. 411–449

P.A. Sturrock (ed.), *Solar Flares: A Monograph From Skylab Solar Workshop II* (1980b)

P.A. Sweet, Annu. Rev. Astron. Astrophys. **7**, 149 (1969)

E. Tandberg-Hanssen, A.G. Emslie, *The Physics of Solar Flares* (Cambridge University Press, Cambridge, 1988), p. 286

G.H.J. van den Oord, Astron. Astrophys. **234**, 496 (1990)

R.F. van Oss, G.H.J. van den Oord, Astron. Astrophys. **299**, 297 (1995)

N. Vilmer et al., Space Sci. Rev. (2011). doi:10.1007/s11214-010-9728-x

S. White et al., Space Sci. Rev. (2011). doi:10.1007/s11214-010-9708-1

V.V. Zharkova, J.C. Brown, D.V. Syniavskii, Astron. Astrophys. **304**, 284 (1995)

V.V. Zharkova et al., Space Sci. Rev. (2011). doi:10.1007/s11214-010-9803-y